

Low-energy properties of the Kondo lattice model

This article has been downloaded from IOPscience. Please scroll down to see the full text article.

2011 J. Phys.: Condens. Matter 23 094212

(<http://iopscience.iop.org/0953-8984/23/9/094212>)

View [the table of contents for this issue](#), or go to the [journal homepage](#) for more

Download details:

IP Address: 212.235.211.101

The article was downloaded on 01/03/2011 at 15:41

Please note that [terms and conditions apply](#).

Low-energy properties of the Kondo lattice model

O Bodensiek¹, R Žitko², R Peters³ and T Pruschke¹

¹ Institute for Theoretical Physics, University of Göttingen, Friedrich-Hund-Platz 1, D-37077 Göttingen, Germany

² J Stefan Institute, Jamova 39, SI-1000 Ljubljana, Slovenia

³ Department of Physics, Graduate School of Science, University of Kyoto, Kitashirakawa-Oiwakecho, 606-8502 Kyoto, Japan

E-mail: pruschke@theorie.physik.uni-goettingen.de

Received 30 July 2010, in final form 22 September 2010

Published 17 February 2011

Online at stacks.iop.org/JPhysCM/23/094212

Abstract

We study the zero-temperature properties of the Kondo lattice model within the dynamical mean-field theory. As an impurity solver we use the numerical renormalization group. We present results for the paramagnetic case showing the anticipated heavy-fermion physics, including direct evidence for the appearance of a large Fermi surface for antiferromagnetic exchange interaction. Allowing for the formation of a Néel state, we observe at finite doping an antiferromagnetic metal below a critical exchange interaction, which shows a crossover from a local moment antiferromagnet with a small Fermi surface for weak exchange coupling to a heavy-fermion antiferromagnet with a large Fermi surface for increasing exchange.

Including lattice degrees of freedom via an additional Holstein term we observe a significant suppression of the Kondo effect, leading to a strongly reduced low-energy scale. For too large electron–phonon coupling we find a complete collapse of the heavy Fermi liquid and the formation of polarons.

(Some figures in this article are in colour only in the electronic version)

1. Introduction

Heavy-fermion systems based on 4f or 5f intermetallics are paradigms for electronic correlations in solid state physics. The low-temperature physics of these compounds is strongly influenced by the local moment on the f shell, subject to an antiferromagnetic exchange to the conduction electrons. The resulting physical properties are, in many cases, again Fermi-liquid-like, however with extremely enhanced Landau parameters, in particular an effective mass up to three orders of magnitude larger than the one found in conventional metals [10, 27, 28]. This large effective mass is the reason why these systems are referred to as *heavy-fermion materials* (HF). Moreover, in addition to these extreme Fermi liquid properties, the HF also show various phase transitions and the thermodynamics show that these transitions actually occur within the heavy Fermi liquid [27]. Finally, the appearance of superconductivity in a system with initially well-defined magnetic moments is a rather unconventional feature, and close investigation revealed early on that the nature of the ordered

state may be rather unconventional [10]. This observation has been substantiated by developments over the past 15 years which showed that a larger number of these HF systems exhibit rather peculiar quantum-phase transitions, partially identified as the driving force behind the superconducting transitions [28, 29].

Other materials which show a coupling between itinerant quasi-particles and localized spins are certain transition metal oxides [13], magnetic semiconductors or semi-metals in the series of rare earth monpnictides and monochalcogenides [21, 26], and diluted magnetic semiconductors such as Ga_{1-x}Mn_xAs [14, 18]. Here, the coupling between local spin and conduction electrons is usually mediated through Hund's exchange and thus typically is ferromagnetic.

A theoretical description of HF compounds is conventionally based on the Kondo lattice model (KLM):

$$H_{\text{KLM}} = \sum_{\vec{k}, \sigma} \epsilon_{\vec{k}} \hat{c}_{\vec{k}, \sigma}^{\dagger} \hat{c}_{\vec{k}, \sigma} - J \sum_i \vec{s}_i \cdot \vec{S}_i. \quad (1)$$

The operators $\hat{c}_{\vec{k}, \sigma}^{(\dagger)}$ denote annihilation (creation) operators of

itinerant quasiparticles with dispersion $\epsilon_{\vec{k}}$, \vec{s}_i is the operator for the conduction states' spin density at lattice site \vec{R}_i and \vec{S}_i describes a spin of magnitude S localized at site \vec{R}_i . The interaction between the spin of the conduction states and the localized spin is modeled as a conventional isotropic exchange interaction J .

The dilute version of the KLM (1), the so-called single-impurity Kondo model (SIKM) where there exists only one additional spin at site $\vec{R}_i = 0$, is well understood and shows for antiferromagnetic coupling $J < 0$ the Kondo effect [12], which precisely leads to the phenomena observed in the Fermi liquid phase of HF systems, namely a strongly enhanced mass. There are nowadays several computational tools to treat the SIKM, for instance continuous-time Monte Carlo [20] or Wilson's numerical renormalization group [4] methods.

In theoretical treatments one usually ignores the lattice degrees of freedom. On the other hand, all the above-mentioned materials have a rather strong electron-phonon coupling [1, 13] and one can expect that the charge physics driven by phonons somehow competes with the spin physics due to the exchange interaction with the localized spin. Moreover, without exchange coupling, phonons will lead to conventional s-wave superconductivity. Thus the investigation of the interplay between a coupling to a spin and the lattice degrees of freedom is very interesting.

This paper is intended to give a summary of the physical properties of the KLM as seen by the dynamical mean-field theory. This necessarily excludes nonlocal phenomena like unconventional superconductivity, but allows for the study of antiferromagnetism and whether it is always accompanied by a breakdown of the large Fermi surface. Inclusion of phonons eventually leads to superconductivity [3], which, however, is of the standard local s-wave type. A detailed account of an investigation of the interplay of phonon-mediated superconductivity and HF physics will be presented elsewhere.

This paper is organized as follows. In section 2 we discuss the model and the approximation used to solve it. The case without phonons, i.e. the conventional heavy-fermion physics both in the paramagnetic and the antiferromagnetically ordered state is the subject of section 3. The effect of phonons on the low-energy properties of superconductivity will be discussed in section 4. A short summary and outlook will close the paper.

2. Model and method

The KLM Hamiltonian (1) will again be the basic model. Except for the one dimension case, no analytical solution exists, and even conventional numerical tools such as quantum Monte Carlo (QMC) become rather cumbersome due to a severe sign problem away from particle-hole symmetry. Thus, a reliable approximate method is needed. If one is not interested in the properties too close to a phase transition or in the rather complicated, nonlocal ordering phenomena, a suitable tool is dynamical mean-field theory (DMFT) [9]. In this method, the lattice is mapped onto an effective single-impurity problem, which can then be solved using standard techniques. Here, we use the numerical renormalization group (NRG) approach [4, 30]. One of its apparent advantages is the

possibility to access small energy scales without difficulty and cover the whole range from $T = 0$ to finite temperatures of the order of the bare energy scales. Furthermore, it also allows us to include phonons to a certain extent, namely an Einstein mode coupled through a Holstein term to the charge degrees of freedom. As is suggested from effects like Kondo volume collapse [1, 13], such a term could be rather important. We will thus work with a Hamiltonian (for a detailed introduction and further references see [24])

$$H = H_{\text{KLM}} + \omega_0 \sum_i b_i^\dagger b_i + g \sum_{i\sigma} (c_{i\sigma}^\dagger c_{i\sigma} - 1)(b_i^\dagger + b_i) \quad (2)$$

where ω_0 is the frequency of an appropriate optical mode and g a measure of the electron-phonon coupling. How such an additional local coupling can be treated within NRG is described in detail in [4]. To obtain reasonably accurate spectra also for higher energies, we use the broadening strategy introduced by [8].

As is well known, one major effect of the Holstein model is to introduce an effective attractive interaction to the electronic subsystem: if the phonon frequency ω_0 and the electron-phonon coupling g become large, keeping g^2/ω_0 constant, the phonons can be integrated out, yielding an attractive local Coulomb interaction $U_{\text{eff}} = -2g^2/\omega_0$. Without an explicit exchange interaction J , one will then obtain a Hubbard model with attractive U , which shows charge density and superconducting ordering phenomena [2, 7]. From the point of view of Kondo physics, the negative U will lead to a Kondo-like behavior in the charge sector, strongly competing with the spin Kondo effect introduced by J . We can thus expect interesting physics to occur when both couplings are present.

3. KLM without phonons

Let us begin with a comprehensive summary of the basics of heavy-fermion physics. We used a 2D square lattice with nearest-neighbor hopping for the conduction states. Note that the DMFT is rather insensitive to the dimensionality and we chose the 2D lattice to facilitate visualization of the results. Calculations were done with an NRG discretization parameter $\Lambda = 2$, between 1000 and 5000 states were kept per NRG step and, where applicable, 50 bosons kept initially. These values were systematically changed for selected calculations to ensure that the results were independent of these numerical parameters.

3.1. Paramagnetic metal

Let us start with a comparison of the properties at finite J , but with $g = 0$. We can distinguish two cases, namely an antiferromagnetic exchange $J < 0$ and a ferromagnetic $J > 0$. The resulting density of states (DOS) for $T = 0$ and $|J|/W = 0.25$ at a filling $n_c = 0.8$ of the conduction band is shown in figure 1. The quantity W denotes the bandwidth of the conduction band and will serve as the energy scale hereafter. There are notable differences between the two cases $J < 0$ and $J > 0$. The DOS for $J > 0$ looks very much like the DOS of the bare conduction band (dotted curve in figure 1),

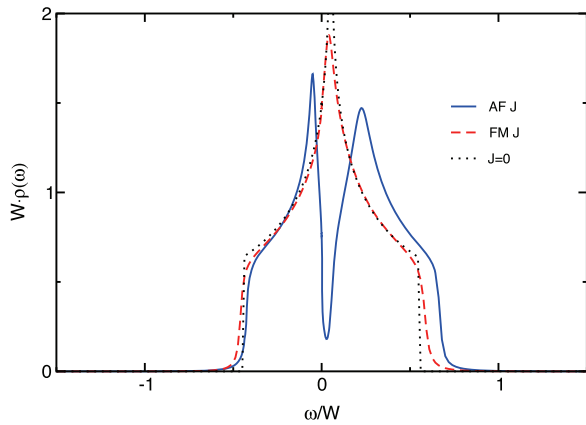


Figure 1. DOS at $T = 0$ for the KLM (1) with $|J| = 0.25W$, where W denotes the bandwidth of the conduction electrons. The filling of the band is $n_c = 0.8$. The dotted curve displays the DOS at $J = 0$ as reference.

although it is somewhat broadened. For $J < 0$, however, the DOS is strongly modified [19], showing a pseudogap close to the Fermi energy $\omega = 0$. This latter feature is a fingerprint of heavy-fermion physics, resulting from a picture of hybridized bands [10]. This interpretation becomes even more apparent when one looks at the spectral function along the standard \vec{k} directions in the first Brillouin zone of the 2D square lattice in figure 2, left panel. A dark color means low intensity, while a bright color means high. Included as a full black line is the bare band structure of the 2D nearest-neighbor tight-binding

band. For $J > 0$ we basically see the band structure of the 2D nearest-neighbor tight-binding band. There is a moderate broadening, which actually is to be expected, because for $J > 0$ the local spin effectively acts as a potential scatterer for the band states [12]. For such a situation the DMFT is equivalent to a CPA calculation, which yields a constant broadening. For $J < 0$ (right panel), on the other hand, there is a flattening of the band structure close to the Fermi energy and a structure similar to a hybridization gap opens. The flat portion of the lower band corresponds to a large effective mass of the quasi-particles. Note that we have a rather sharp structure at the Fermi energy, i.e. one can indeed talk about quasi-particles here.

Another remarkable difference between the cases $J > 0$ and $J < 0$ is observed when one looks at the momentum distribution function $n(\vec{k})$ displayed in the right part of figure 2. As already noted for the spectral functions, the result for $J > 0$ resembles the Fermi function, slightly smeared out by incoherent scattering from the spins. In any case, the Fermi surface is located at the \vec{k}_F of a non-interacting 2D tight-binding band with a filling $n_c = 0.8$. On the other hand, the momentum distribution for $J < 0$ does not show any distinct features at this particular value of \vec{k} . Instead, one notes a small jump in $n(\vec{k})$ at a vector outside the square marking the Fermi surface of a half-filled system. A closer inspection shows that this \vec{k} vector corresponds to a Fermi surface of a system with $n_c = 1.8$, i.e. the system shows a ‘large’ Fermi surface with the spin degrees of freedom now contributing to the quasiparticles. Note that the height of the jump in $n(\vec{k})$ is directly related to the inverse effective mass of the quasiparticles.

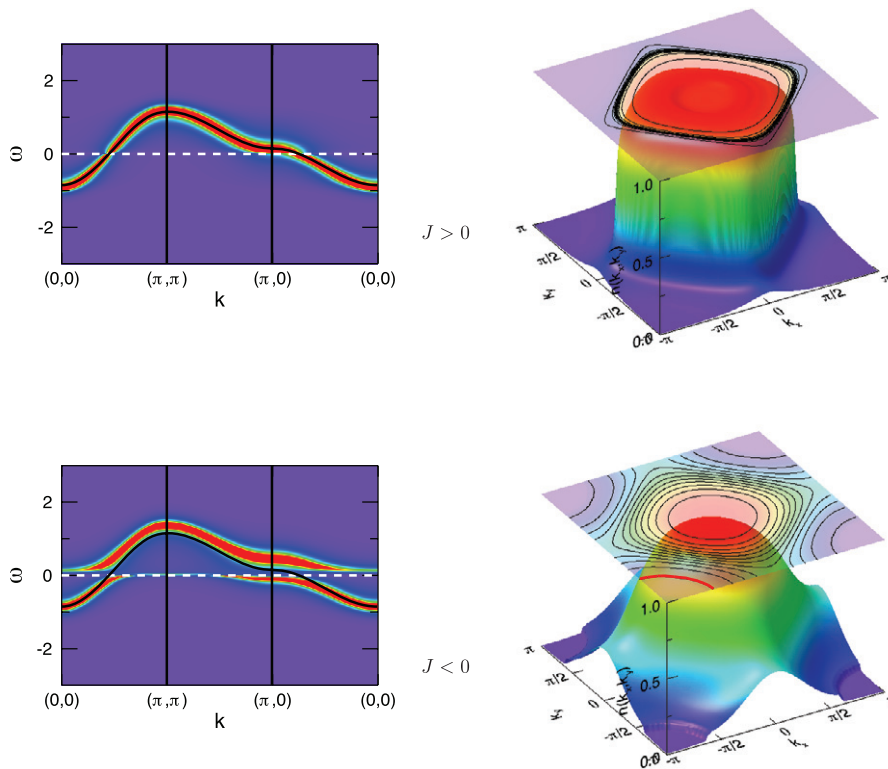


Figure 2. Spectral functions (left) and momentum distribution (right) for $|J| = 0.25W$, other parameters are as in figure 1. The thick line in the lower left corner of the contour plot for $J < 0$ denotes the position of the jump in the momentum distribution.

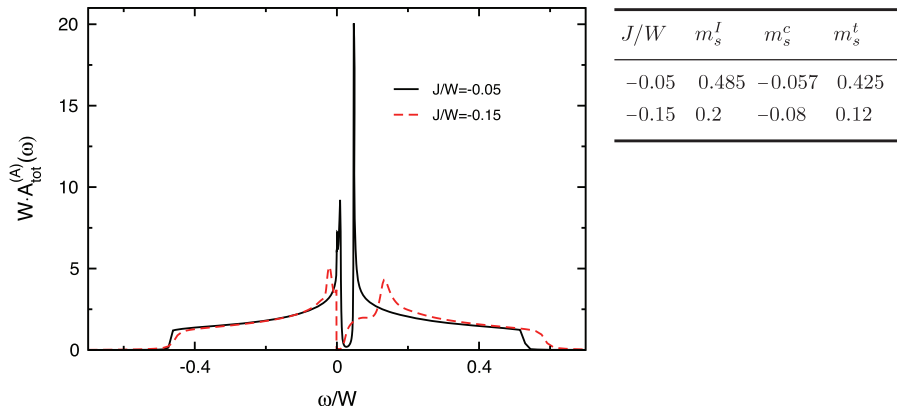


Figure 3. Total DOS for the A sublattice at $T = 0$ for $J/W = -0.05$ (full line) and $J/W = -0.15$ (dashed line). The table shows the staggered magnetizations.

The results for $J < 0$ in figure 2 represent the essence of HF physics, namely the generation of heavy quasiparticles, represented by flat bands with a structure known from hybridized bands and a large Fermi surface.

3.2. Antiferromagnetic ordering

As is well known, the Kondo lattice model shows a variety of magnetically ordered states [6, 11, 15, 16]. Within DMFT, an overview was presented in [5, 22]. The major findings at $T = 0$ are that at half-filling (Kondo insulator regime) one finds a critical $J_c < 0$, with no magnetic phases present for $J < J_c$ and antiferromagnetism for $J > J_c$. The staggered magnetization of local spins and band electrons are opposite for $J < 0$, leading to an effectively reduced total moment especially close to the ‘quantum critical’ point. Note that this effect is enhanced when one includes interactions in the band electron system (see, e.g., [22]).

Away from half-filling there appear, at strong enough doping, ferromagnetic phases in addition [22, 25]. For $J < J_c$, no further magnetic phase was observed in the vicinity of half-filling. For $J > J_c$, one can, however, again stabilize antiferromagnetic phases. For example, for a filling $n_c = 0.9$ of the conduction band, such an ordered state is found for $J \lesssim -W/4$. To obtain a reasonable convergence and a stable solution, the DMFT calculations must be done with Broyden mixing [31]. Quite interestingly, we are not able to find stable and reasonably converged solutions for $-0.125 \lesssim J/W \lesssim -0.1$. The results for $J/W = -0.05$ and -0.15 are shown in figure 3 together with a table of the values for the staggered magnetization of the local spin, m_s^I , the conduction band, m_s^c , and their sum, m_s^t . A rather interesting question related to this is whether the ordered state corresponds to a ‘local moment’ regime, i.e. where the local spins are effectively decoupled from the band states and one has a small Fermi surface, or if it is a ‘heavy-fermion’ magnet with a large Fermi surface. The most interesting case, of course, is when both appear as a function of J and there might be a phase transition associated with the change in Fermi surface topology. Obviously, inspection of the DOS in figure 3 alone is not sufficient to identify a possible transition.

Such information can, however, be obtained by inspecting the spectral function. The results are shown in figure 4, where the k vectors are now restricted to the first magnetic Brillouin zone (see, for example, [23]). Included in the figure as a continuous black line is the dispersion calculated with the Hartree term of the self-energy alone [17]. This curve thus represents the proper approximation for the situation of ordered local moments polarizing the Fermi sea. The left part shows the overall structures and the right part a magnified view of the region around the Fermi energy.

Quite clearly, the concept of a small Fermi surface, i.e. ordered local spins polarizing the band states, describes the situation very well for $J/W = -0.05$. The situation changes completely for $J/W = -0.15$. First, the staggered magnetization has dropped to $m_s \approx 0.12$ now, with $m_s^I \approx 0.2$ and $m_s^c \approx -0.08$ (see the table in figure 3). Thus, while the polarization of the band states has not changed significantly, the one for the local spins has dropped by more than 50%. Further increasing $|J|$ does not lead to any new features. The polarizations of both local moments and band electrons smoothly drop to zero for $J/W \approx -W/4$. Second, the spectral function has become much more HF-like with a flat band around Γ (cf figure 2). Therefore, the scenario of a decoupled Fermi sea and local moment ordering surely does not apply any more. In fact, the whole system looks much more band-like, with a large Fermi surface⁴. This scenario is also supported by the fact that, for increasing coupling $|J|$, the system more strongly shows tendencies to rather form spin density waves than Néel order. These observations strongly hint towards a phase transition from a local moment-like phase at small $|J|$ to a phase where magnetic ordering appears in the heavy quasiparticles at larger $|J|$. However, a decisive answer as to what type of phase transition this is at present cannot be given.

4. Effect of phonons

An extended account of the effect of Einstein phonons on HF physics is given in [24], where we concentrated on the

⁴ Note that ‘large’ in the magnetic Brillouin zone means centered around Γ , as the M point has been mapped back to the zone center.

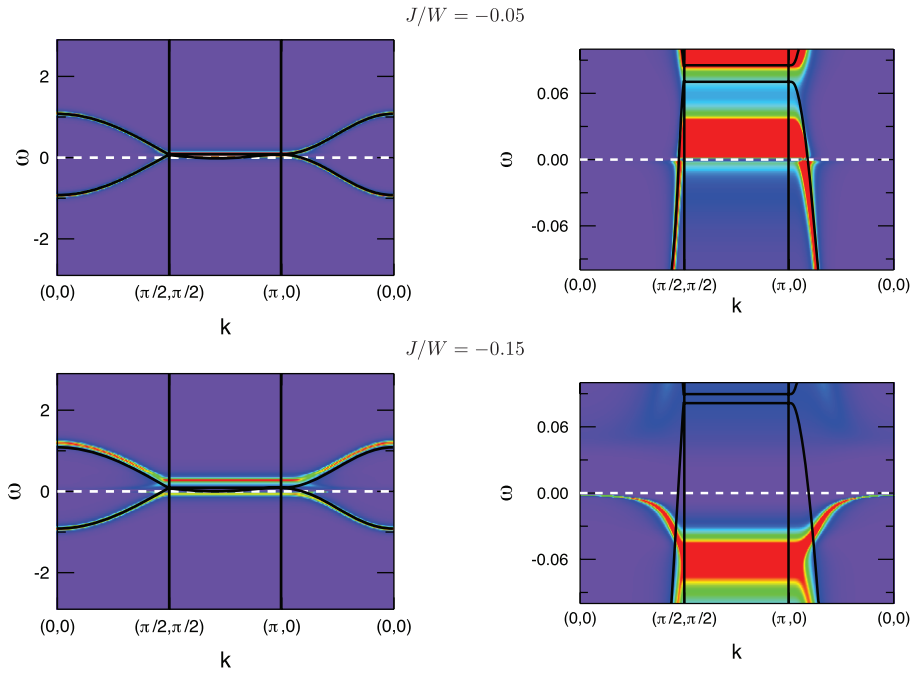


Figure 4. Spectral functions for \vec{k} from the magnetic Brillouin zone for $n_c = 0.9$. Left: full energy range. Right: magnified view around the chemical potential.

periodic Anderson model. Here, we show further results for the KLM, which supplement the findings reported there, in particular the behavior as the Kondo effect collapses due to polaron formation. We restrict the discussion here to $J < 0$ and fix the phonon frequency to $\omega_0 = 0.5W$. Calculations were done for $J = -0.5W$ at a filling $n_c = 0.8$. The values for ω_0 and J are apparently rather large. However, smaller J and ω_0 do not change the qualitative picture, but make it much harder to visualize the structures.

The results are summarized in figure 5 for $g = 0, 0.2W$ and $0.4W$. The first thing to note is that the phonons lead to a reduction of the width of the pseudogap close to the Fermi energy and also a reduction of the overall bandwidth. In addition, there occur new structures at higher energy with increasing electron-phonon coupling, which are related to the formation of polarons. The reduction of the overall bandwidth is expected and can be interpreted as an increase of the effective mass of the bare conduction states due to the coupling to the phonons. The reduction of the width of the pseudogap, on the other hand, signals a likewise reduction of the low-energy scale generated by the Kondo effect. Both effects lead to an effective mass as a function of g as depicted in the inset to figure 5. Note that m^* initially depends only weakly on g . However, it diverges very strongly as $g \rightarrow \omega_0$.

These features become more apparent by inspecting the spectral functions in figure 6. Both effects, the overall reduction of the bare bandwidth and the increased HF mass, are clearly visible. Moreover, with increasing g one finds roughly \vec{k} -independent structures representing the polaronic modes. Further increasing g , we observe a rather sharp crossover around $g \approx \omega_0$ to a completely incoherent behavior. The results of a calculation for $g = \omega_0$ are shown in figure 7. Note that there is no Kondo feature left either in the DOS

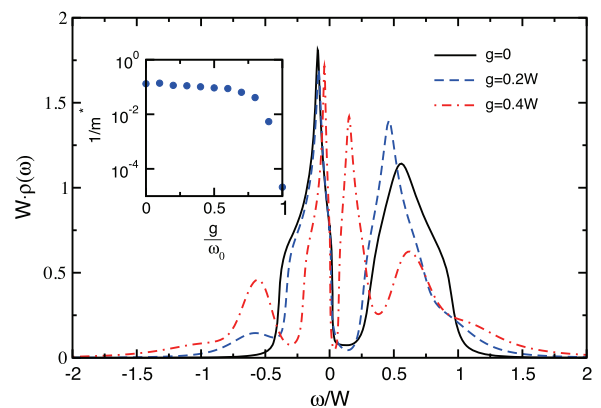


Figure 5. DOS at $T = 0$ for the KLM (1) with $J = -0.5W$ and $g = 0, 0.2W$ and $0.4W$. The filling of the band is $n_c = 0.8$. The inset shows the dependence of the effective mass on g .

or in the spectral function and all structures are rather broad. We would also like to mention that for $g \gtrsim \omega_0$ it becomes increasingly hard to stabilize a given occupation $n \neq 0, 1, 2$ of the conduction band. This indicates that the system is close to a Peierls instability, i.e. the formation of a charge density wave together with a lattice distortion.

5. Summary

We have presented a summary of properties of the Kondo lattice model within dynamical mean-field theory at $T = 0$ using the numerical renormalization group as an impurity solver. We have extended the Kondo lattice model by including an Einstein mode coupled to the electrons via a Holstein

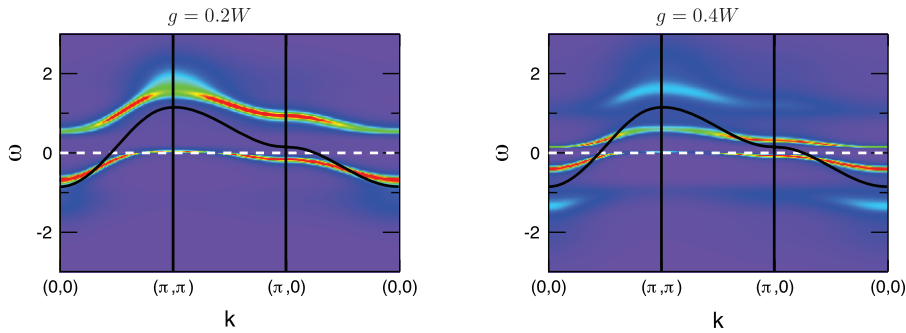


Figure 6. Spectral functions for $J = -0.5W$, other parameters are as in figure 5.

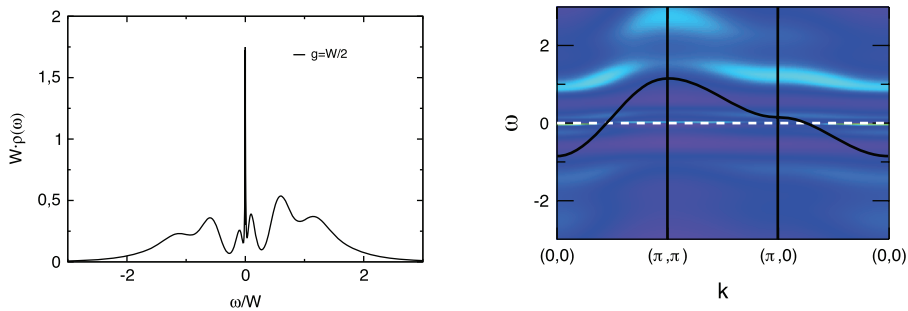


Figure 7. DOS (left panel) and spectral function (right panel) for $g = 0.5W = \omega_0$. Other parameters are as in figure 5.

term. The importance of such modes for HF materials can be deduced from strong effects such as the Kondo volume collapse observed in Ce.

Without the phonons, we find for antiferromagnetic coupling the expected heavy-fermion behavior, with hybridized bands appearing in the spectrum and a large Fermi surface. For ferromagnetic coupling, on the other hand, the bare band structure is only weakly modified due to incoherent scattering from the local degrees of freedom.

Allowing for a magnetically ordered state, we are able to stabilize a Néel order for $J > J_c$, where $J_c < 0$ depends on the filling of the conduction band. For the case $n_c = 0.9$ discussed here, we find $J_c/W \approx -0.25$. Quite interestingly, there appears to be a qualitative difference between the ground-state for $|J| \rightarrow 0$ and $|J| \rightarrow |J_c|$. In the former case, the results can be well interpreted with a system consisting of local moments which order antiferromagnetically via an RKKY-like exchange. In this case, we have a small Fermi surface and the band states are weakly polarized by the presence of the local moments. For the latter case we find a rather different behavior. First, although the polarization of the local moments is considerably smaller than for small J , the band polarization has actually increased, pointing towards a much stronger entanglement between local spins and conduction electrons. Second, the spectral functions again form flat bands around points of the magnetic Brillouin zone which map to the heavy-fermion bands without Néel order. A more detailed investigation of the crossover with respect to transitions could not yet be accomplished due to convergence problems of the DMFT in the interesting region.

Adding phonons, we find a general narrowing of the bare band, which also leads to a reduction of the Kondo scale.

Eventually, when the coupling becomes of the order of the phonon frequency, the electrons tend to localize and form polarons with the phonons. At that point, the effective mass diverges and the electronic spectrum becomes incoherent. As a side observation we note that in this region one sees a tendency of the system to form a charge density wave.

The results for $T = 0$ presented here strongly motivate further investigations, in particular at finite T , searching for the critical temperature and in particular the interplay between HF and local moment physics with respect to magnetism, charge ordering and superconductivity.

Acknowledgments

We wish to acknowledge helpful discussions with Andreas Honecker, Akihisa Koga, Achim Rosch, Fakhre Assaad and Dieter Vollhardt. RP wants to thank the Japan Society for the Promotion of Science (JSPS) together with the Alexander von Humboldt Foundation for a postdoctoral fellowship. Computer support was provided by the Gesellschaft für wissenschaftliche Datenverarbeitung in Göttingen and the Norddeutsche Verbund für Hoch- und Höchstleistungsrechnen.

References

- [1] Allen J W and Martin R M 1982 *Phys. Rev. Lett.* **49** 1106
- [2] Bauer J, Hewson A C and Dupuis N 2009 *Phys. Rev. B* **79** 214518
- [3] Bodensiek O, Pruschke T and Žitko R 2010 *J. Phys.: Conf. Ser.* **200** 012162
- [4] Bulla R, Costi T A and Pruschke T 2008 *Rev. Mod. Phys.* **80** 395

- [5] Chattopadhyay A, Millis A J and Sarma S D 2001 *Phys. Rev. B* **64** 012416
- [6] Fazekas P and Müller-Hartmann E 1991 *Z. Phys. B* **85** 285
- [7] Freericks J K, Jarrell M and Scalapino D J 1993 *Phys. Rev. B* **48** 6302–14
- [8] Freyn A and Florens S 2009 *Phys. Rev. B* **79** 121102
- [9] Georges A, Kotliar G, Krauth W and Rozenberg M J 1996 *Rev. Mod. Phys.* **68** 13
- [10] Grewe N and Steglich F 1991 *Handbook on the Physics and Chemistry of Rare Earths* ed J K A Gschneidner and L Eyring (Amsterdam: North-Holland) p 343
- [11] Henning S and Nolting W 2009 *Phys. Rev. B* **79** 064411
- [12] Hewson A C 1993 *The Kondo Problem to Heavy Fermions (Cambridge Studies in Magnetism)* (Cambridge: Cambridge University Press)
- [13] Imada M, Fujimori A and Tokura Y 1998 *Rev. Mod. Phys.* **70** 1039
- [14] Jungwirth T, Sinova J, Masek J, Kucera J and Macdonald A H 2006 *Rev. Mod. Phys.* **78** 809–64
- [15] Kienert J and Nolting W 2006 *Phys. Rev. B* **73** 224405
- [16] Lacroix C and Cyrot M 1979 *Phys. Rev. B* **20** 1969
- [17] Negele J and Orland H 1988 *Quantum Many-Particle Physics* (Reading, MA: Addison-Wesley)
- [18] Ohno H 1998 *Science* **281** 951–6
- [19] Otsuki J, Kusunose H and Kuramoto Y 2009 *Phys. Rev. Lett.* **102** 017202
- [20] Otsuki J, Kusunose H, Werner P and Kuramoto Y 2007 *J. Phys. Soc. Japan* **76** 114707
- [21] Ovchinnikov S 1991 *Phase Transit.* **36** 15
- [22] Peters R and Pruschke T 2007 *Phys. Rev. B* **76** 245101
- [23] Pruschke T and Zitzler R 2003 *J. Phys.: Condens. Matter* **15** 7867
- [24] Raczkowski M, Zhang P, Assaad F F, Pruschke T and Jarrell M 2010 *Phys. Rev. B* **81** 054444
- [25] Santos C and Nolting W 2002 *Phys. Rev. B* **65** 144419
- [26] Sharma A and Nolting W 2006 *J. Phys.: Condens. Matter* **18** 7337–48
- [27] Stewart G R 1984 *Rev. Mod. Phys.* **56** 755
- [28] Stewart G R 2001 *Rev. Mod. Phys.* **73** 797
- [29] von Löhneysen H, Rosch A, Vojta M and Wölfle P 2007 *Rev. Mod. Phys.* **79** 1015
- [30] Wilson K G 1975 *Rev. Mod. Phys.* **47** 773
- [31] Žitko R 2009 *Phys. Rev. B* **80** 125125